

Simulations of fluidelastic forces and fretting wear in U-bend tube bundles of steam generators: Effect of tube-support conditions

Marwan Hassan^{*1} and Atef Mohany²

¹*School of Engineering, University of Guelph, Guelph, Ontario, Canada*

²*Department of Mechanical Engineering, University of Ontario Institute of Technology, Oshawa, Ontario, Canada*

(Received May 30, 2014, Revised August 8, 2014, Accepted August 20, 2014)

Abstract. The structural integrity of tube bundles represents a major concern when dealing with high risk industries, such as nuclear steam generators, where the rupture of a tube or tubes will lead to the undesired mixing of the primary and secondary fluids. Flow-induced vibration is one of the major concerns that could compromise the structural integrity. The vibration is caused by fluid flow excitation. While there are several excitation mechanisms that could contribute to these vibrations, fluidelastic instability is generally regarded as the most severe. When this mechanism prevails, it could cause serious damage to tube arrays in a very short period of time. The tubes are therefore stiffened by means of supports to avoid these vibrations. To accommodate the thermal expansion of the tube, as well as to facilitate the installation of these tube bundles, clearances are allowed between the tubes and their supports. Progressive tube wear and chemical cleaning gradually increases the clearances between the tubes and their supports, which can lead to more frequent and severe tube/support impact and rubbing. These increased impacts can lead to tube damage due to fatigue and/or wear at the support locations. This paper presents simulations of a loosely supported multi-span U-bend tube subjected to turbulence and fluidelastic instability forces. The mathematical model for the loosely-supported tubes and the fluidelastic instability model is presented. The model is then utilized to simulate the nonlinear response of a U-bend tube with flat bar supports subjected to cross-flow. The effect of the support clearance as well as the support offset are investigated. Special attention is given to the tube/support interaction parameters that affect wear, such as impact and normal work rate.

Keywords: flow-induced vibrations; fluidelastic instability; impact; friction; loosely-supported tubes; nuclear steam generators

1. Introduction

Flow-induced vibrations of heat-exchanger tubes is identified as one of the most significant safety issues in operating nuclear steam generators. These issues are manifested in the form of failures due to fatigue and fretting wear at the supports. Such failures can be very expensive in the case of nuclear steam generators. Therefore, flow-induced vibrations have been the subject of extensive research in the past five decades to understand the phenomenon and to establish

*Corresponding author, E-mail: mahassan@uoguelph.ca

guidelines for the design and safe operation of these devices. The vibrations are excited by several excitation mechanisms. Turbulence and fluidelastic instability are the two dominant mechanisms in most heat exchangers (Païdoussis 1983, Weaver and Fitzpatrick 1988). Fluidelastic instability is considered to be the most destructive mechanism and is characterized by the evolution of large amplitude oscillations when the flow velocity exceeds a certain threshold. If this threshold is exceeded, tubes may fail catastrophically in a short period of time. A detailed description of this mechanism can be found in the work of Price (1995). In order to avoid such failures counter measures, such as limiting the flow velocity and stiffening the tube structure, are considered. Therefore, supports are installed to provide a stiffer tube configuration. Tube/support assemblies are usually loose-fitting to accommodate tube thermal expansion and to facilitate the manufacturing and the assembling process. However, the existence of these supports allows for impacting and sliding against the support to take place. This in turn results in fretting wear damage potential at the tube support locations. The prevention of such failures can be obtained by careful design with proper selection of tube supports bars especially in the U-bend region. Nevertheless, some situations may arise from worn or ill-positioned supports. This may result in larger than usual tube/support gaps. In such a case the tube may be exposed to high levels of impact and sliding force due to both turbulence and fluidelastic coupling forces induced by the cross-flow. Prediction of tube response under the conditions of loose supports and fluidelastic force are a very complex process due to the nonlinearity of both the tube boundary conditions (loose supports) and the fluidelastic forces. Predicting such wear requires temporal records of quantities such as the impact forces and the tube response. This paper deals with such predictive analyses, and attempts to present a simulation for a full U-bend tube configuration. The work also presents a systemic assessment of the determination of the appropriate number of anti-vibration bars in the U-Bend region. Moreover, the effect of support offset on the dynamic response of the U-bend configuration is also investigated.

2. Modelling

A loosely supported tube which is subjected to turbulence and fluidelastic force is described by the following equation

$$[M]\{\ddot{w}\} + [C]\{\dot{w}\} + [K]\{w\} = \{F_{turb}(t)\} \quad (1)$$

where $w(t)$ is the response of the tube, M is the total mass, C is the damping coefficient, K is the system stiffness, and F_{turb} is the turbulence excitation force. Matrices M , C , and K contain the contributions of the fluid flow and the contact at the support. Due to the loose supports, the system stiffness and damping are nonlinear. One approach to model of the system involves splitting the working space into two regions (states) within which the system behaves linearly. Therefore, the nonlinearity will represent the transition from one state to another. It is possible to separate the flow and contact contributions to the system matrices in the form of forces and move it to the right-hand side of the above equation as follows

$$[M_s]\{\ddot{w}\} + [C_s]\{\dot{w}\} + [K_s]\{w\} = \{F_{turb}(t) + F_f(t) + F_{pre}(t)\} \quad (2)$$

In the above equation, K_s and C_s represent the structural components of the system while M_s

contains both the structural, internal flow added mass, and external flow added mass. $F_f(t)$ and $F_{turb}(t)$ are the fluidelastic forces and the turbulence excitation forces, respectively. In some cases, the external forces also have an additional constant component (preload, $F_{pre}(t)$) to represent the steady drag force and tube/support offset. In general the tube structure is discretized using finite elements.

The mathematical treatments of the impact force range from discretizing both the tube and each support using beam and plate elements, and applying a generalized overlap and contact algorithm to a much more efficient specialized algorithm utilizing a localized tube deformation effect. The latter method will be utilized here and was described in full detail by Hassan *et al.* (2002). However, a brief description is presented in this section. Loose supports can be modelled by a number of massless bars attached by an equivalent contact spring and damper (Fig. 1). Impact takes place when the normal displacement component at the support location exceeds the tube support gap. In such an event, a corrective force is estimated based on the overlap displacement and applied as an external force to the system. The normal contact force (F_{cn}) is given by

$$\begin{aligned} F_{cn} &= F_{spr} + F_{dmp} & \text{for } w_n > C_r, & \text{ and} \\ F_{cn=0} & & \text{for } w_n < C_r, & \end{aligned} \quad (3)$$

where F_{spr} and F_{dmp} are the spring and damping forces while C_r is the radial clearance. During the tube support contact, friction arises if the tube is excited to move in a tangential direction to the support. Several models have been developed to deal with a steam generator's tube bundle friction. These models include the Velocity Limited Friction Model (VLFM), the Spring Damper Friction Model (SDFM), and the Force Balance Friction Model (FBFM). A detailed description and comparison of these models can be found in the work of Hassan and Rogers (2005). In the current work, the FBFM is used with a velocity feedback algorithm.

As mentioned earlier turbulence excitation is a significant vibration mechanism that determines the long term life of the tubes. Deep within the tube bundle, tubes are excited by the turbulence generated within the bundle, which is in turn governed by the tube bundle geometry. In general, fluid excitation due to turbulence is modelled as randomly distributed forces. The bounding power spectral density (PSD) measured by Oengören and Ziada (1998) for a tube array of pitch-to-diameter ratio (P/d) of 1.61 was utilized in this work to generate the time-domain fluid forces. It is a common approach to excite the system through a fully correlated turbulence force along the entire tube length. However, such an assumption is not entirely accurate and is overly conservative. The correlation length of the turbulent forces is typically a few diameters. A less conservative approach is to use a number of random forces, assuming a full correlation within each tube span – see, for instance, Hassan *et al.* (2003). The power spectral density (PSD) of the dynamic force acting on any element is expressed as

$$S_{FF} = \frac{1}{4} \rho_f^2 d^3 U^3 l^2 \phi, \quad (4)$$

where ρ_f , U , and ϕ are the fluid density, the pitch flow velocity, and the spectral bound of the turbulence forces, respectively. For triangular arrays with small spacing, the spectral bound for the lift ϕ_L and drag ϕ_D directions are given by

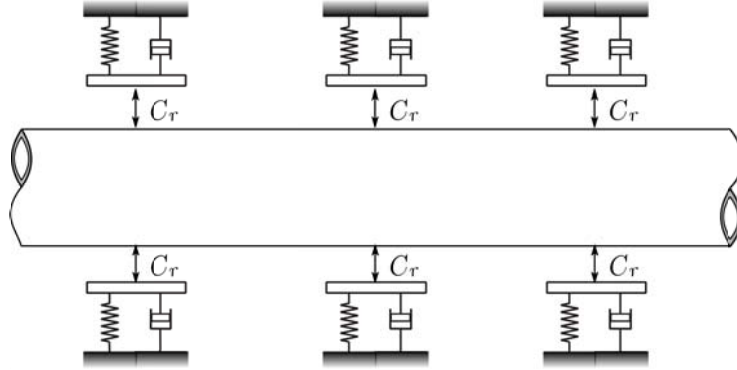


Fig. 1 Tube-support model

$$\begin{aligned}
 \phi_L &= 4.75 \times 10^{-3} \left(\frac{fd}{U} \right)^{-0.4} \quad \text{for} \quad \frac{fd}{U} < 0.43, \\
 \phi_L &= 1.02 \times 10^{-4} \left(\frac{fd}{U} \right)^{-0.5} \quad \text{for} \quad \frac{fd}{U} > 0.43, \\
 \phi_D &= 7.35 \times 10^{-4} \left(\frac{fd}{U} \right)^{-0.4} \quad \text{for} \quad \frac{fd}{U} > 0.53, \text{ and} \\
 \phi_D &= 3.96 \times 10^{-5} \left(\frac{fd}{U} \right)^{-0.5} \quad \text{for} \quad \frac{fd}{U} > 0.53.
 \end{aligned} \tag{5}$$

Fluidelastic instability forces are modelled using the time domain formulation introduced by Hassan *et al.* (2010, 2011). In this formulation, the complex flow through a tube array is approximated by several flow cells. Each flow cell consists of an active tube (flexible) attached to two flow channels and a number of boundary tubes (fixed), as shown in Fig. 2(a). The flow in each flow channel can be effectively modelled as a one-dimensional inviscid flow using a curvilinear coordinate (s), which originates at the centre of the active tube and extends to the flow cell inlet. The active tube affects the channel flow through the contact region from the attachment location (s_a) to the separation point (s_s). While the original formulation of the flow cell model (Lever and Weaver 1982) assumes that the tube is vibrating at a steady-state amplitude at a frequency close to the natural frequency of the tube, the current model does not contain such restrictions and allows the tube to respond to both turbulence and fluidelastic instability (FEI) forces. This is also very suitable for the case of loosely supported tubes, which tend not to have a well-defined natural frequency, complicating the response prediction. The flow inside the channel is solved to predict the velocity and the pressure fields as a result of deformation to the flow channels caused by the motion of the tube. The solution algorithm involves decomposing the parameters of the flow channel (channel area A , flow velocity U , and pressure P) into first order terms ($\bar{A}, \bar{U}, \bar{P}$) and

second order terms (a, u, p) as follows:

$$\begin{aligned} A(s, t) &= \bar{A}(s) + a(s, t), \\ U(s, t) &= \bar{U}(s) + u(s, t), \text{ and} \\ P(s, t) &= \bar{P}(s) + p(s, t). \end{aligned} \tag{6}$$

The first order terms (steady) are related to the geometry of the flow channel while the second order terms (perturbations) are related to the motion of the flexible tube. The area perturbation can be directly calculated from the tube vibration time history as follows

$$a(s, t) = w(t - \tau(s)) \cdot \hat{e}_t \cdot f(s) \tag{7}$$

τ is the time lag required for the flow to respond to the tube motion and can be attributed to the process of flow redistribution and momentum. This process is thought to be caused by the flow inertia (Lever and Weaver, 1982), flow retardation (Price and Païdoussis 1984), or vorticity convection and dissipation (Granger and Païdoussis, 1996). More discussion can be found in the work of El Bouzidi and Hassan (2015) regarding the time lag formulation. Now using the one dimensional continuity and momentum equations along the length of the flow channel, an expression describing the flow velocity and the pressure perturbations for a fluid of density ρ can be derived as follows

$$u(s, t) = \frac{-1}{\bar{A} + a(s, t)} \left[U(-S_0) \cdot a(s, t) + \int_{-S_0}^S \frac{\partial a(s, t)}{\partial t} ds \right], \text{ and} \tag{8}$$

$$p(s, t) = P(-S_0) + \rho \left\{ \frac{1}{2} U(-S_0)^2 - \frac{1}{2} U^2 - \int_{-S_0}^S \frac{\partial U}{\partial t} ds \right\} - \rho \left\{ \frac{h}{2S_0} \cdot \int_{-S_0}^S U^2 ds \right\}. \tag{9}$$

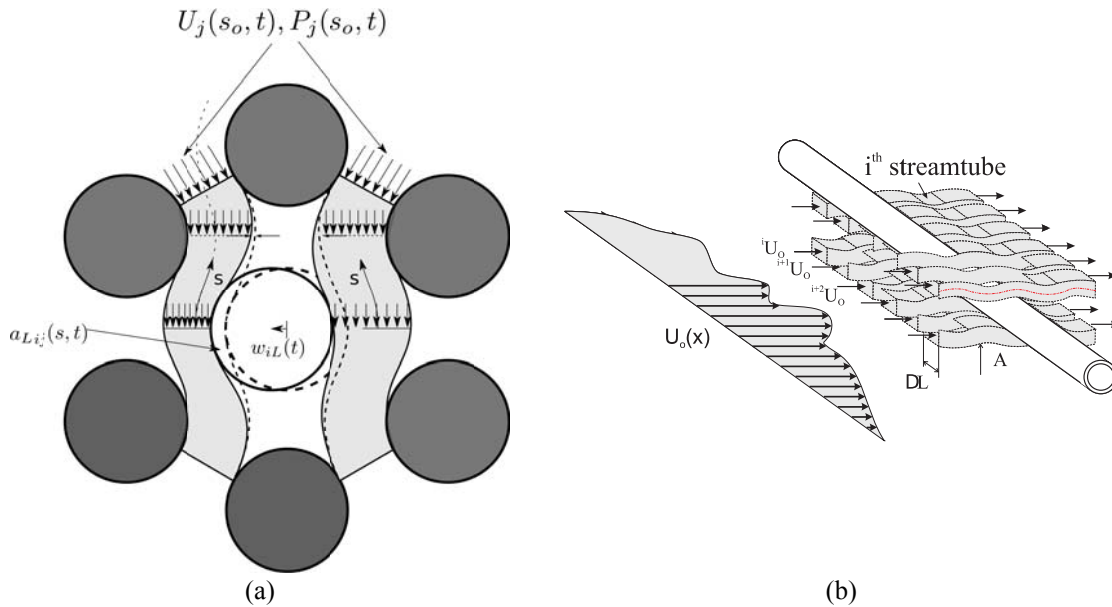


Fig. 2 The flow dell model

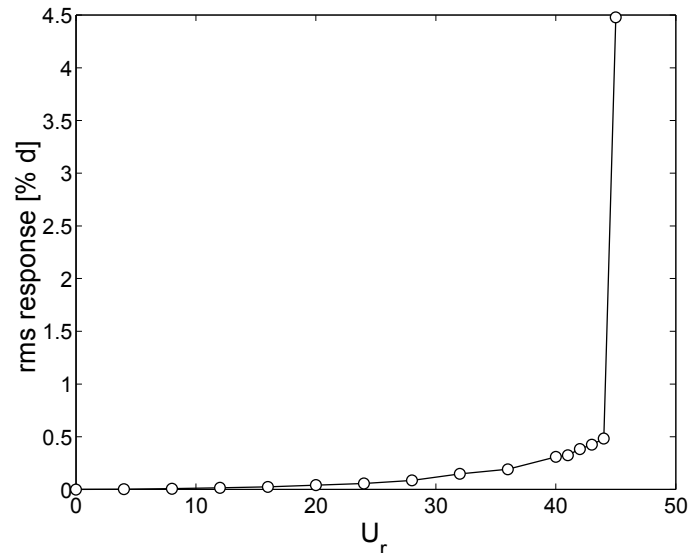


Fig. 3 Linear tube response

The inlet velocity $U(-S_o)$ and pressure $P(-S_o)$ are considered to be constant. The parameter h accounts for the resistance due to viscous losses. A reasonable estimate of the resistance coefficient can be obtained by assuming that it does not vary significantly with the Reynolds number in the vicinity of the stability threshold for each array (Lever and Weaver 1986). It was also shown that h does not greatly influence the stability threshold of the system. Therefore, an average value of 0.275 was used for all simulations. Additional effects, such as the flow separation oscillation, can be introduced which requires the modeling of the boundary at the tube/flow channel interface (Anderson *et al.* 2014).

To demonstrate the model, a simplified one-degree of freedom system is utilized. The system parameters, such as tube diameter, stiffness, and mass, are 0.01905 m, 1039.2 N/m, and 0.66 kg, respectively. The tube is subjected to air cross-flow. The above algorithm, including the turbulence and FEI excitation, were implemented and the time integration was conducted using the Newmark technique. Fig. 3 shows the tube response as a function of the velocity. The rms tube response is expressed as a percentage of the tube diameter while the flow velocity is normalized by the tube diameter and the natural frequency ($U_r = U/fd$). The response gradually increases as the flow velocity increases up to a reduced flow velocity of 44. During this range of flow velocity, the response is dominated by the random forces due to the turbulence effect. Beyond a reduced flow velocity of 44 an abrupt increase in the response takes place as a result of the system crossing the FEI stability threshold. Both FEI and turbulence are affecting the tube response. However, the relative contribution of each component varies depending on the proximity to the stability threshold.

Detailed implementation procedure of the above model in a general-purpose finite element code INDAP (Incremental Nonlinear Dynamic Analysis Program) was described in detail by Hassan and Mohany (2013). In this implementation, each finite element is attached to a flow cell identical to that shown in Fig. 2(a). The depth of the flow cell matches the element length (d_l) as shown in Fig. 2(b). For each element, the history of the average displacement component in the lift direction

is used to calculate the instantaneous channel area perturbation, $a(s, t)$. The calculated area perturbation and the inlet flow velocity for the element are then utilized to calculate the perturbation velocity along the channel. The momentum equation is then solved along the flow channel to calculate the pressure perturbation, which is integrated along the tube/channel interface to calculate the destabilizing FEI forces. These FEI forces along with the random forces due to turbulence are added to the global force vector, and the system's equation is then solved to obtain the response.

2. Simulation parameters

Four different U-bend configurations were simulated. Each tube configuration was modeled by means of 91 three-dimensional beam elements, each of which has 12 DOF, as shown in Fig. 4(a). The tube geometrical and material properties are listed in Table 1.

Table 1 Material and geometrical properties

	Parameter	Value
Geometrical Properties	Straight Leg Length	L=7 m
	U-bend radius	1.9 m
	Outside Diameter	$d_o = 19$ mm
	Inside Diameter	$d_i = 15.5$ mm
	Array	Parallel Triangle P/d=1.5
Material Properties	Modulus of Elasticity	E=200 GPa
	Density	$\rho = 8304$ kg/m ³
	Poisson's Ratio	$\nu = 0.28$

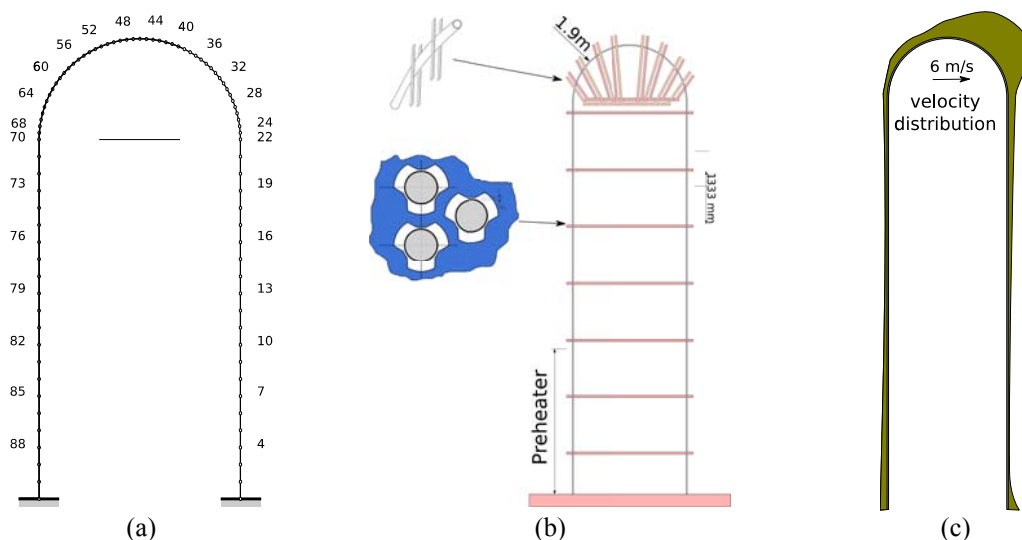


Fig. 4 U-bend tube model: (a) FE nodes along the U-bend, (b) Tube broached hole and flat bar supports and (c) The flow distribution in the U-bend region

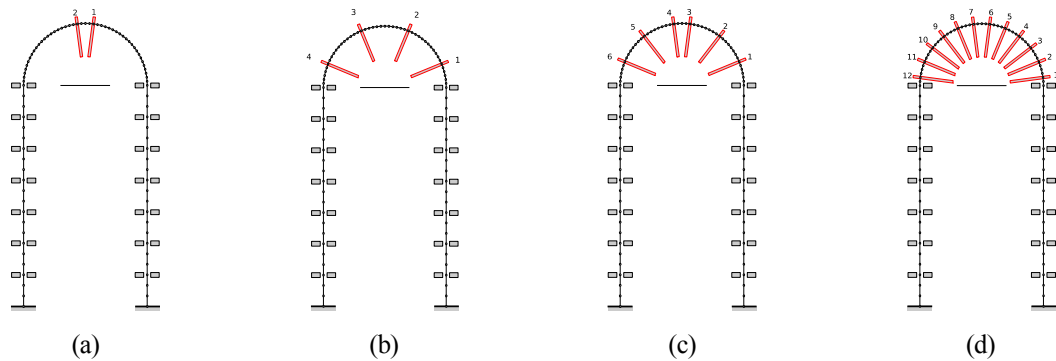


Fig. 5 U-bend tube configurations: (a) Configuration 1, (b) Configuration 2, (c) Configuration 3 and (d) Configuration 4

Each tube is supported by 7 tube sheet supports (broached hole supports) in the hot and the cold leg, as shown in Fig. 4(b). The differences between these configurations lie in the number and locations of the flat bar supports (Fig. 5). Typical flow distribution in the U-bend can be found in the work of Mohany *et al.* (2012). Such flow distribution was adopted in this work. Configurations 1, 2, 3, and 4 have 2, 4, 6, and 12 flat bar supports, respectively, as shown in Fig. 5. For each configuration, the clearance between the tube and the flat bar supports was varied between 0.1 mm to 1.0 mm. Each simulation was run for 10 sec with a time step of 0.01 msec. The rms streamwise and transverse responses of the tube were determined. In addition, the impact forces and the normal work rate were calculated.

3. Results

Fig. 6 shows the rms tube response for the transverse and streamwise directions for Configurations 2, 3, and 4. Configuration 1 was found to be fluidelastically unstable resulting in a very large tube response and extremely high impact force levels. Therefore, the results of Configuration 1 were omitted from this section. Figure 6 shows the response for a clearance of 1.0 mm. The transverse response shows peaks at the mid-spans and valleys of the supports especially for the hot leg (nodes 1-20) and cold leg (nodes 60-91); refer to Fig. 4(a). For all configurations, the transverse response has its highest values in the U-bend region where the anti-vibration bars are located. Configuration 2 exhibits the highest transverse response with values up to 6% of the tube diameter, while the lowest response was found for Configuration 4. In addition, the response of Configuration 4 is almost flat in the U-bend region. This can be attributed to the large number of flat bars used. In general, the streamwise response is much smaller than the transverse response. However, Configuration 4 shows a higher streamwise response than the transverse counterpart.

Fig. 7 shows the rms impact force at the U-bend anti-vibration bars for two sets of support clearances (0.1 mm and 1.0 mm). The anti-vibration bars were numbered 1, 2, 3, etc. starting from the hot side and moving counterclockwise towards the cold side (see Fig. 5). For all configurations the impact force level is higher for larger support clearances. The highest level of impact force was found in Configuration 2 (Fig. 7(a)). When higher numbers of supports were used, the impact

force level was lowered. In addition, using more anti-vibration bars increased the ratio of the impact force level for the large and small clearances. Moreover, using more supports yielded a better distribution of the impact force across the anti-vibration bars.

Normal work is one of the most important parameters that is utilized to estimate the fretting wear potential. The normal work rate is defined as the normal component of the contact force, F_{cn} , integrated over the sliding distance, w_s . As shown in Fig. 8, similar trends are manifested in the case of the impact force level, and the normal work rate lowers as the number of supports is increased. For the clearance case of 1.0 mm, the predicted normal work rate of Configuration 2 is in the range of 45 to 70 mW. These are considered extremely high values as well-designed steam generators are expected to have work rate levels in the range of a few mW. Configuration 3 also exhibits high values of work rate for a clearance of 1.0 mm. However, for the case of 0.1 mm the work rate is much lower (about 10 mW).

From the above results, high and undesirable values of impact forces and normal work rates can be observed for a lower number of anti-vibration bars. With only 2-4 bars, Configurations 1 and 2 would not represent a viable design option. Configurations 3 and 4 with 6-12 bars seem to exhibit reasonable normal work rate values with Configuration 3 being a borderline case.

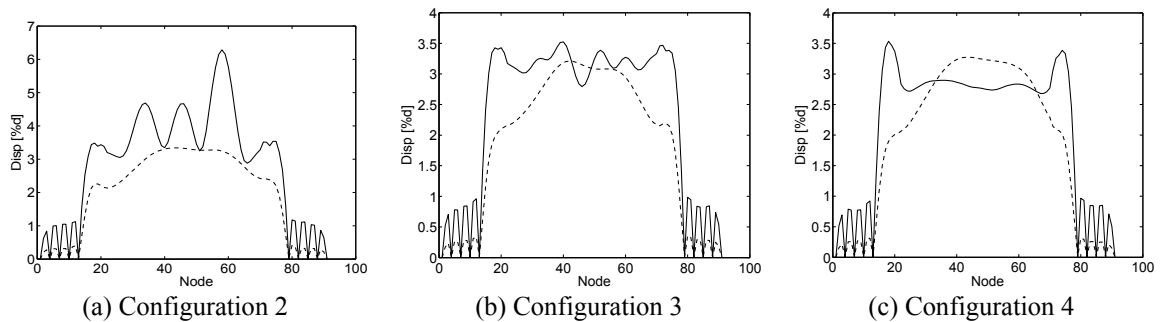


Fig. 6 Streamwise (dotted line) and transverse (solid line) response along the tube nodes

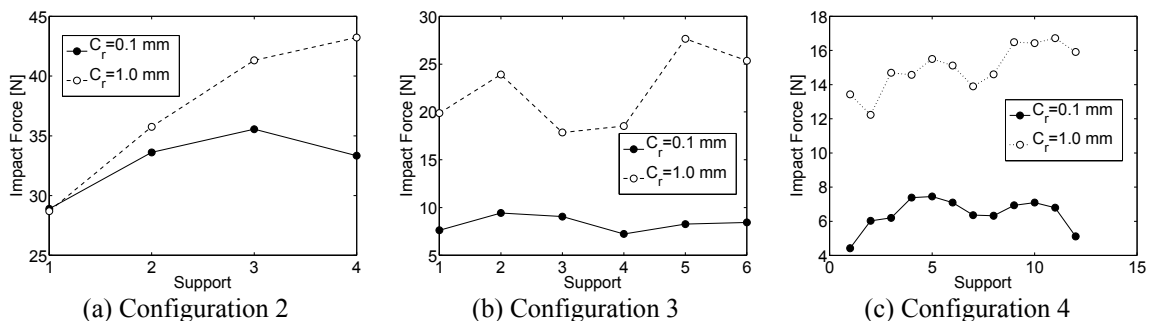


Fig. 7 Rms impact force at the supports located in the U-bend

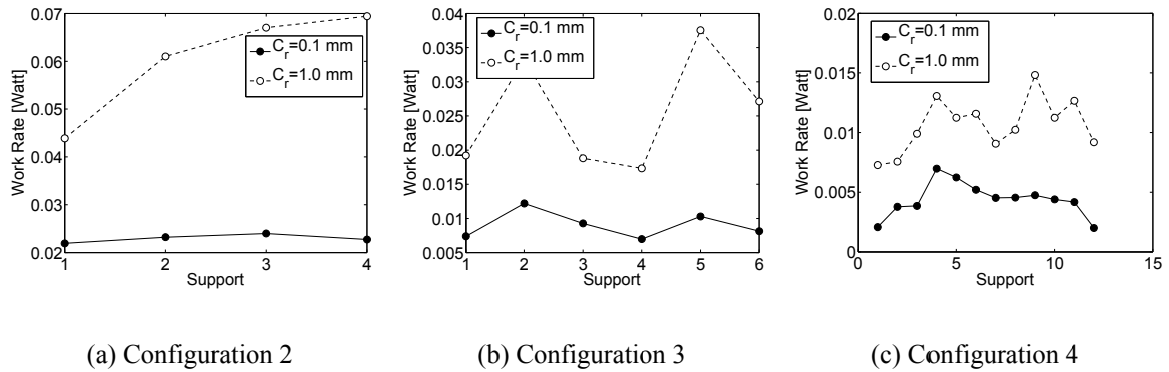


Fig. 8 Normal work rate at the supports located in the U-bend

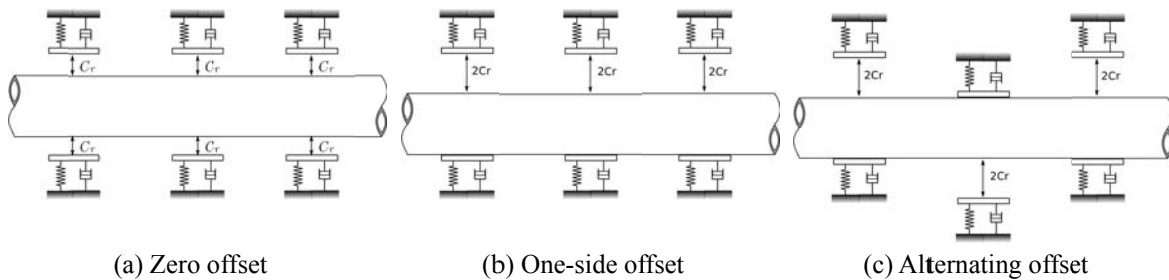


Fig. 9 Tube support offset types

Since perfectly aligned supports are more difficult to achieve, as they require tighter clearances and excellent manufacturing techniques, the more likely scenario is having supports with some form of offset between them. Therefore, in this work an attempt to investigate the effect of support offset is made. Configuration 3 will be utilized in this study as it has a marginal performance. Three offset cases were studied and are shown in Fig. 9. The offset scenarios are applied to the anti-vibration bars located in the U-bend region. Comparisons in terms of value increase in the response, impact force, or normal work rate will always be in reference to the baseline case, which is the zero offset.

Fig. 10 shows the tube response along the tube length for the three offset cases. The transverse response was greatly reduced for the alternate offset case. The reduction is particularly large in the neighborhood of the U-bend apex. Using the one-sided offset seems to increase the transverse response. Similarly, introducing the alternate support offset results in the largest reduction in the streamwise response. The greatest reduction is about 66% around the apex of the U-bend. However, about a 20% increase in the tube response is obtained when using the one-sided offset.

The effect of the offset scenario on the rms impact forces is shown in Fig. 11. Results are shown for two clearance cases; small (0.1 mm) and large (1.0 mm). For the small clearance case (Fig. 11(a)), introducing the one-sided offset has little influence on the predicted impact force. However, the introduction of the alternate offset results in an increase in the impact force. The increase is greatest at Supports 3 and 4 which are close to the top of the U-bend region.

Introducing a one-sided offset results in a significant decrease in the impact force for the large clearance case. The reduction is in the range of 30% to 50% for Supports 3-5. A significant increase in the impact force in the two middle supports (3 and 4) was predicted when the alternate offset was introduced. However the side supports (1, 2, 5, and 6) experience smaller impact force levels.

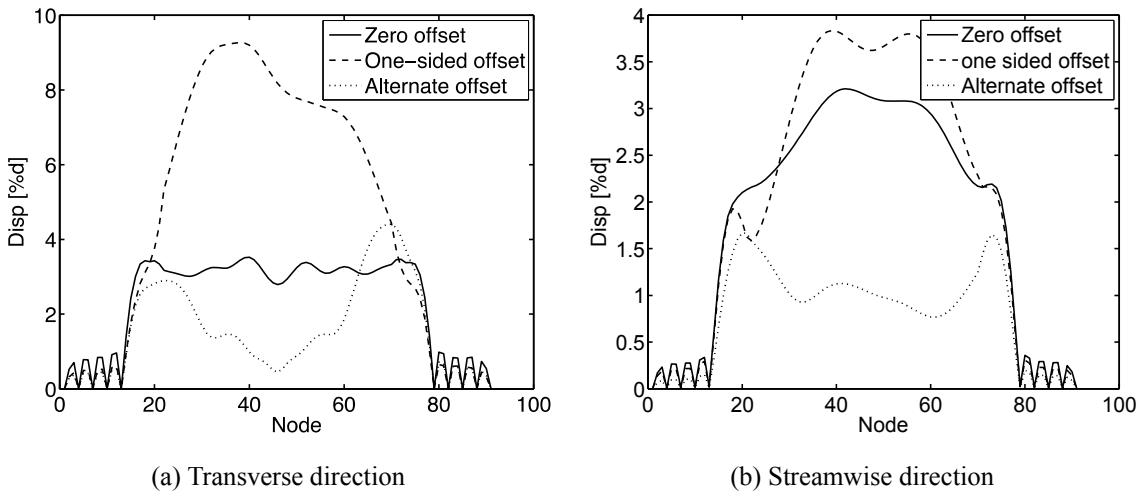


Fig. 10 The effect of the support offset on the response along the tube nodes

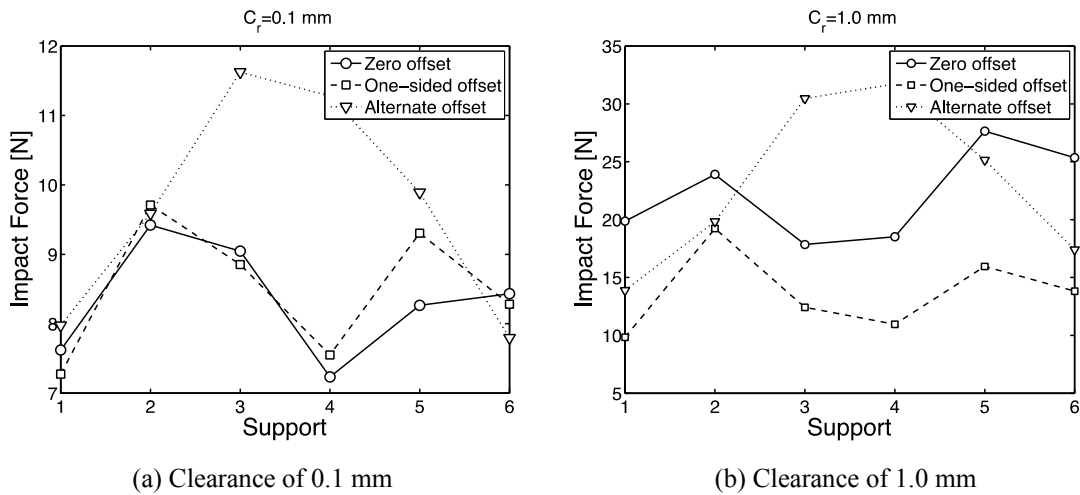


Fig. 11 The effect of the support offset on the rms impact force

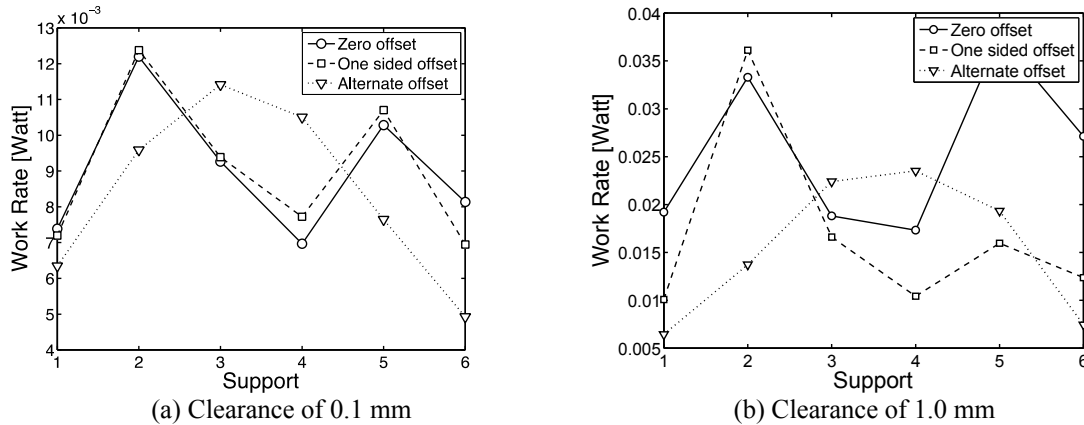


Fig. 12 The effect of the support offset on the normal work rate

A prediction of the normal work rate for the two clearance cases is shown in Fig. 12. Small differences in the normal work rate level were predicted when introducing the one-sided offset for the small clearance. An increase in the normal work rate for Supports 3 and 4 was observed for the alternate offset case (Fig. 12(a)). Introduction of an offset is shown to have an attenuating effect on the work rate for the large clearance (Fig. 12(b)).

The predicted response, impact force, and normal work rate show the complexity of the dynamic system and its sensitivity to the conditions at the supports in terms of the clearance and the offset conditions. For example, the alternate offset conditions result in a relatively large impact force at the top of the U-bend region, which provides a larger contact force and a larger friction capacity. Increasing the friction capacity allows the means of energy dissipation. This large energy dissipation takes place at the top of the U-bend region, which provides the maximum moment arm and hence, a greater effectiveness. Conversely, the one-side offset results in a lower impact force level, especially for the large clearance value (Fig. 11(b)). Smaller impact force levels limit the available friction capacity of the system. This in turn leads to a larger streamwise response (Fig. 10(b)). Hence, certain combinations of support clearance and offset conditions could promote larger streamwise oscillations and could even result in instability. This would explain some of the recent failures, which took place in tube bundles in newly manufactured nuclear steam generators.

5. Conclusions

Simulations of a full scale U-Bend tube bundle were carried out. The simulations modelled the structural dynamics of the tube including the effect of loose supports. Modelling of the fluidelastic instability excitation was presented. Simulations were conducted for four configurations with 2, 4, 6, and 12 anti-vibration bars installed in the U-bend region. For the rated flow velocity and the density distribution used, Configuration 1 is unstable while Configuration 4 (with 12 supports) is stable with safe normal work rate levels. While the use of 4 anti-vibration bars seems to provide stability, the normal work rates predicted are very high. Such a configuration can not be used. The

third configuration was also stable with a relatively high normal work rate. Introducing the offset at the anti-vibration bars seems to be beneficial in reducing the response, impact force and normal work rates for large clearances. Little benefit can be gained from a support offset if the clearance between the tube and its support is tight. In fact, for small clearances such an offset might result in a higher tube response. The proposed model and the simulation results can be helpful in the design and prediction of flow-induced vibration of tube bundles in nuclear steam generators.

Acknowledgments

The research described in this paper was financially supported by the Natural Science Foundation.

References

- Anderson, B., Hassan, M. and Mohany, A. (2014), "Modelling of fluidelastic instability in a square inline tube array including the boundary layer effect", *J. Fluid. Struct.*, **48**, 362-375.
- El Bouzidi, S. and Hassan, M. (2015), "An investigation of time lag causing fluidelastic instability in tube arrays", *J. Fluid. Struct.*, **57**, 264-276.
- Granger, S. and Païdoussis, M.P. (1996), "An improvement to the quasi-steady model with application to cross-flow-induced vibration of tube array", *J. Fluid Mech.*, **320**, 163-184.
- Hassan, M. and Mohany, A. (2013), "Fluidelastic instability modelling of loosely supported multi-span u-tubes in nuclear steam generators", *J. Press. Vessel Technol. - ASME*, **135**, 011306.
- Hassan, M. and Rogers, R. (2005), "Friction modelling of preloaded tube contact dynamics", *Nuclear Eng. Des.*, **235**, 2349-2357.
- Hassan, M., Gerber, A. and Omar, H. (2010), "Numerical estimation of fluidelastic instability in tube arrays", *J. Press. Vessel Technol. - ASME*, **132** (4), 041307.
- Hassan, M.A., Rogers, R.J. and Gerber, A.G. (2011), "Damping-controlled fluidelastic instability forces in multi-span tubes with loose supports", *Nuclear Eng. Des.*, **241**(8), 2666-2673.
- Lever, J.H. and Weaver, D.S. (1982), "A theoretical model for the fluidelastic instability in heat exchanger tube bundles", *J. Press. Vessel Technol. - ASME*, **104**, 104-147.
- Lever, J. and Weaver, D. (1986), "On the stability of heat exchanger tube bundles, part ii: Numerical results and comparison with experiments", *J. Sound Vib.*, **107**(3), 393-410.
- Mohany, A. Janzen, V., Feenstra, P. and King, S. (2012), "Experimental and numerical characterization of flow-induced vibration of multi-span U-tubes", *J. Press. Vessel Technol. - ASME*, **134**, 011301.
- Oengören, A. and Ziada, S. (1998), "An in-depth study of vortex shedding, acoustic resonance and turbulent forces in normal triangle tube arrays", *J. Fluid. Struct.*, **12**, 717-758.
- Price, S.J. (1995), "A review of theoretical models for fluidelastic instability of cylinder arrays in cross-flow", *J. Fluid. Struct.*, **9**, 463-518.
- Païdoussis, M. (1983), "A review of flow-induced vibrations in reactors and reactor components", *Nuclear Eng. Desi.*, **74**(1), 31-60.
- Weaver, D. and Fitzpatrick, J. (1988), "A review of crossflow induced vibrations in heat exchanger tube arrays", *J. Fluid. Struct.*, **2**, 73-93.